



Article

# *Bacillus velezensis* Identification and Recombinant Expression, Purification and Characterization of Its Alpha-Amylase

Xiaodong Zhang <sup>1,2,†</sup>, Caixia Li <sup>1,†</sup>, Xuantong Chen <sup>2</sup>, Chonlong Chio <sup>2</sup>, Sarita Shrestha <sup>2</sup> and Wensheng Qin <sup>2,\*</sup>

<sup>1</sup> Food and Pharmacy College, Xuchang University, Xuchang 461000, China; zxd95@xcu.edu.cn (X.Z.); 20201009@xcu.edu.cn (C.L.)

<sup>2</sup> Department of Biology, Lakehead University, Thunder Bay, ON P7B5E1, Canada; xchen24@lakeheadu.ca (X.C.); cchio@lakeheadu.ca (C.C.); sshrest4@lakeheadu.ca (S.S.)

\* Correspondence: wqin@lakeheadu.ca

† These authors contribute to this article equally.

**Abstract:** Amylases account for about 30% of the global market of industrial enzymes, and the current amylases cannot fully meet industrial needs. This study aimed to identify a high  $\alpha$ -amylase producing bacterium WangLB, to clone its  $\alpha$ -amylase coding gene, and to characterize the  $\alpha$ -amylase. Results showed that WangLB belonged to *Bacillus velezensis* whose  $\alpha$ -amylase gene was 1980 bp coding 659 amino acids designated as BvAmylase. BvAmylase was a hydrophilic stable protein with a signal peptide and a theoretical pI of 5.49. The relative molecular weight of BvAmylase was 72.35 kDa, and was verified by SDS-PAGE. Its modeled structure displayed that it was a monomer composed of three domains. Its optimum temperature and pH were 70 °C and pH 6.0, respectively. It also showed high activity in a wide range of temperatures (40–75 °C) and a relatively narrow pH (5.0–7.0). It was a Ca<sup>2+</sup>-independent enzyme, whose  $\alpha$ -amylase activity was increased by Co<sup>2+</sup>, Tween 20, and Triton X-100, and severely decreased by SDS. The  $K_m$  and the  $V_{max}$  of BvAmylase were  $3.43 \pm 0.53$  and  $434.19 \pm 28.57$  U/mg. In conclusion, the  $\alpha$ -amylase producing bacterium WangLB was identified, and one of its  $\alpha$ -amylases was characterized, which will be a candidate enzyme for industrial applications.

**Keywords:** *Bacillus velezensis*; alpha-amylase; recombinant expression; purification; characterization

**Citation:** Zhang, X.; Li, C.; Chen, X.; Chio, C.; Shrestha, S.; Qin, W.

*Bacillus velezensis* Identification and Recombinant Expression, Purification and Characterization of Its Alpha-Amylase. *Fermentation* **2021**, *7*, 227. <https://doi.org/10.3390/fermentation7040227>

Academic Editor: Jean-Luc Legras

Received: 29 August 2021

Accepted: 4 October 2021

Published: 11 October 2021

**Publisher's Note:** MDPI stays neutral with regard to jurisdictional claims in published maps and institutional affiliations.



**Copyright:** © 2021 by the authors. Licensee MDPI, Basel, Switzerland. This article is an open access article distributed under the terms and conditions of the Creative Commons Attribution (CC BY) license (<http://creativecommons.org/licenses/by/4.0/>).

## 1. Introduction

Alpha-amylase (EC 3.2.1.1) is a kind of liquefying and endo-amylase which randomly hydrolyze the internal  $\alpha$ -1, 4-glucosidic bond of starch, glycogen, and related polysaccharides to generate dextrin and a small part of reducing sugar [1]. Because the hydroxyl group configuration of the terminal residue of the reducing sugar produced is  $\alpha$ , this hydrolase is called  $\alpha$ -amylase [2].  $\alpha$ -amylase comes from a wide range of sources, such as plants, animals, and microorganisms, and mainly exists in aleurone cells of germinated grains [3,4]. It is an important starch hydrolase and one of the oldest and most widely used enzymes in industrial production [5]. It can be prepared by microbial fermentation or extracted from plants. The properties of  $\alpha$ -amylase from different sources are different. In industry, it is mainly produced by bacteria and fungi due to its stability and higher catalytic activity [6].

Alpha-amylase was first commercialized in 1984 as a drug adjuvant for the treatment of digestive disorders. Now,  $\alpha$ -amylase has been widely used in food, detergent, beer brewing, textile, alcohol, and paper industries [7]. In addition,  $\alpha$ -amylase is used in pharmaceutical, biofuel production, and environmental remediation [7,8]. The increasing demand in various industries requires enzymes with suitable characteristics, therefore, the discovery of new  $\alpha$ -amylases and improvement of the existing ones are of interest.

Alpha-amylase belongs to the glycoside hydrolase 13 (GH13) family, and most of them are  $\text{Ca}^{2+}$ -dependent enzymes. The typical structure of  $\alpha$ -amylase is composed of three domains: Domain A is in the N-terminal, composed of eight  $\alpha$ -helices and eight  $\beta$ -strands linked by loops, forming an  $(\alpha/\beta)_8$  barrel; Domain B protrudes from the surface of the barrel and is located in the third  $\alpha$ -helix and the third  $\beta$ -strand; Domain C is located at the C-terminal, composed of antiparallel  $\beta$ -strands [9,10].

Previously, an  $\alpha$ -amylase producing bacterium named “WangLB” was isolated in our laboratory and it belonged to *Bacillus* with high  $\alpha$ -amylase activity [11]. However, this bacterium was not precisely identified and the sequence of its  $\alpha$ -amylase was unknown which has greatly hindered its application in biotechnology and industries. This paper describes the identification of bacterium by 16S rDNA alignment and biochemical traits, cloning and analyzing the  $\alpha$ -amylase encoding gene and expressing the gene with a Histidine tag at the N-terminal. Finally, the structure of its coding protein was predicted, and the recombinant enzyme was purified and characterized.

## 2. Materials and Methods

### 2.1. Extraction of Genomic DNA from WangLB Bacterium

WangLB strain was an  $\alpha$ -amylase producing bacterium strain preserved in our laboratory. Extraction of genomic DNA was carried out according to our laboratory’s protocol. It was first streaked on Luria-Bertani (LB) solid plate and incubated at 37 °C overnight. Then, single clone was picked by the sterilized toothpick, and inoculated into the liquid LB medium. After being cultured with shaking at 200 rpm for 24 h, 3 mL of the bacteria was centrifuged for 10 min at 9600× *g*, and 564  $\mu\text{L}$  of 1× TE buffer (10 mM Tris-HCl, 1 mM EDTA, pH 8.0) was added to resuspend the pellet. Then, 30  $\mu\text{L}$  of 10% SDS and 6  $\mu\text{L}$  of protease K (10 mg/mL) were added and gently mixed, incubated at 37 °C for 1 h. Then, 100  $\mu\text{L}$  of NaCl (5 M/L) was added and gently mixed to incubate at 65 °C for 2 min. Then, 80  $\mu\text{L}$  of CTAB/NaCl (10% (w/v) CTAB, 0.7 M NaCl) was added, gently mixed, and incubated at 65 °C for 10 min. An equal volume (about 800  $\mu\text{L}$ ) of phenol/chloroform/isoamyl alcohol (v:v:v = 25:24:1) was added, gently mixed, and centrifuged at 9600× *g* for 5 min. Again, the supernatant was transferred into a new centrifuge tube, and an equal volume (about 800  $\mu\text{L}$ ) of chloroform/isoamyl alcohol (v:v = 24:1) was added, gently mixed, and centrifuged at 16,000× *g* for 5 min. The supernatant was transferred to a new centrifuge tube, and 0.7 times the volume of isopropanol (about 560  $\mu\text{L}$ ) was added to precipitate genomic DNA. The centrifuge tube was gently inverted six times. After keeping at room temperature for 10 min, it was centrifuged at 16,000× *g* for 15 min. The DNA pellet obtained after centrifugation was washed with 500  $\mu\text{L}$  of 70% ethanol twice and then air-dried for 5 min, dissolved in 25  $\mu\text{L}$  of 1× TE buffer with RNase A (20  $\mu\text{g}/\text{mL}$ ), incubated at 37 °C for 30 min. Finally, the genomic DNA was stored at −20 °C until use.

### 2.2. Identification of WangLB Bacterium by 16S rDNA

The 16S rDNA of WangLB bacteria was amplified by *Taq* DNA polymerase with a universal eubacterial primer set: 27F (5'-FAGAGTTTGATCmTGGCTCAG-3') and 1492R (5'-TACGGYTACCTTGTTACGAC-3'). The 25  $\mu\text{L}$  reaction system contained *Taq* DNA polymerase (5 U/ $\mu\text{L}$ , Fermentas, Burlington, ON, Canada) 0.5  $\mu\text{L}$ , 10× *Taq* DNA polymerase buffer 2.5  $\mu\text{L}$ , dNTPs (10 mM) 0.5  $\mu\text{L}$ ,  $\text{MgCl}_2$  (25 mM) 1.5  $\mu\text{L}$ , forward and reverse primers (10  $\mu\text{M}$ ) 1  $\mu\text{L}$ , respectively, the genomic DNA template 2  $\mu\text{L}$ , and ddH<sub>2</sub>O 16  $\mu\text{L}$ . The PCR was performed by MyCycler (Bio-Rad, Hercules, CA, USA) and the parameters were: pre-denaturation at 94 °C for 5 min, denaturation at 94 °C for 30 s, followed by annealing at 55 °C for 30 s, extending at 72 °C for 90 s for 30 cycles and finally incubated at 72 °C for 5 min. The PCR products were separated by 1.2% (w/v) of agarose gel electrophoresis. The target fragments were cut from the gel and recycled by a gel extraction kit (Biobasic, Markham, ON, Canada). Then, the concentration of the 16S rDNA was measured by nanodrop2000c (Thermo Scientific, Waltham, MA, USA), and was ligated into the

pUCm-T vector (Biobasic, Markham, ON, Canada). Then, again it was transformed into *Escherichia coli* (*E. coli*) JM109 competent cell, and spread on LB + Amp (Ampicillin, 100 mg/L) + IPTG (Isopropyl  $\beta$ -D-Thiogalactoside, 24 mg/L) + X-gal (5-Bromo-4-chloro-3-indolyl  $\beta$ -D-galactopyranoside, 40 mg/L) agar plate. After that, six white clones were picked and inoculated into LB + Amp (100 mg/L) medium, and cultured for 12 h. The plasmids were extracted using the EZ-10 Spin Column Plasmid DNA Miniprep Kit (Biobasic, Markham, ON, Canada). The extracted plasmids were verified by *EcoRV* (NEB, Beverly, MA, USA) digestion. Finally, the positive clones were sent for DNA sequencing (Eurofins Genomics, Toronto, ON, Canada).

The 16S rDNA sequence of WangLB was BLASTed against the 16S ribosomal RNA sequence database with the default parameters. Some sequences of high similarity with 16S rDNA of WangLB were used to construct the phylogenetic tree. MEGA X was used and the maximum likelihood algorithm was selected to construct the tree with 1000 bootstraps and nucleotide Tamura-Nei substitution model.

### 2.3. Morphological and Biochemical Identification of the WangLB Bacterium

WangLB strain was first streaked on LB solid plate and incubated at 37 °C for 24 h. The colony morphology was observed by naked eyes and magnifying glass. The single colony was picked with a sterilized toothpick and inoculated into 3 mL of sterilized 0.45% (w/v, pH 7.0) of NaCl in a transparent polystyrene tube (12 mm  $\times$  75 mm). The turbidity of the homogeneous WangLB bacterial suspension was measured by VITEK 2 DensiCHEK Plus (bioMérieux, Marcy l'Etoile, France) to make sure the turbidity was between 1.80 to 2.20. Then, the suspension tube and the VITEK 2 BCL card (bioMérieux, Marcy l'Etoile, France) were put into the cardholder. Additionally, the cardholder was put into the filling bin for filling. After filling, the cardholder was transferred into the loading cabin for testing.

### 2.4. Alpha-Amylase Activity Assay

The recombinant  $\alpha$ -amylase activity was determined by the 3,5-dinitrosalicylic acid (DNS) method [11]. Ten microliters of the crude or purified enzyme were added into 100  $\mu$ L of 1% (w/v) starch in 100 mM phosphate buffer (pH 6.0), gently mixed, and incubated at 40 °C or optimum temperature for 20 min. Then, the reaction was stopped by the addition of 300  $\mu$ L of DNS and the mixture was boiled for 5 min. After the mixture was cooled to room temperature, 200  $\mu$ L of the solution was transferred into a 96-well plate to read  $A_{540}$  by Epoch Microplate Spectrophotometer (Biotek, Winooski, VT, USA). Instead of the 10  $\mu$ L of the enzyme, 10  $\mu$ L of sterilized water was used as control. All experiments were repeated at least three times. One unit of enzyme activity was defined as the amount of enzyme that generates 1  $\mu$ M of reducing sugar as maltose per minute under assay conditions.

### 2.5. Cloning and Prokaryotic Expression Vector Construction of *BvAmylase* Gene

In order to figure out the high  $\alpha$ -amylase activity of WangLB bacterium, a pair of gene-specific primers (BvamyaseBamHI-F: CAAGGATCCATGTTTGA AAAACGAT-TCAAACCTC, BvamyaseXhoI-R: ATTCTCGAGATGCGGAAGATAAC-CATTCAAACC, underlines indicate the restriction site) was designed according to the genome of *Bacillus velezensis* FZB42 and other related species. The *BvAmylase* gene was amplified with the genomic DNA of the WangLB bacterium. The reaction system was 20  $\mu$ L containing repliQa HiFi ToughMix (Quantabio, Beverly, MA, USA, 2 $\times$  reaction buffer containing optimized concentrations of MgCl<sub>2</sub>, dNTPs and proprietary formulated HiFi polymerase, hot start antibodies and ToughMix chemistry) 12.5  $\mu$ L, BvamyaseBamHI-F (10 mM) 1  $\mu$ L, BvamyaseXhoI-R (10 mM) 1  $\mu$ L, genomic DNA 2  $\mu$ L, and nuclease-free water 8.5  $\mu$ L. The protocol was 98 °C 10 s, 63 °C 5 s, and 68 °C 8 s for 30 cycles. The PCR product was recycled by a gel extraction kit. The purified PCR product and the plasmid

pET21a were double digested by *Bam*HI (NEB, Beverly, MA, USA) and *Xho*I (NEB, Beverly, MA, USA) for 4 h, separated by 1% agarose gel electrophoresis, and recovered. They were ligated by T4 DNA ligase to get the recombination plasmid pET21a-BvAmylase. The ligation products were transformed into *E. coli* JM109 competent cells and spread on a solid LB + Amp (100 mg/L) plate. The single clones were picked and inoculated into liquid LB + Amp (100 mg/L), shaken for 12 h. Then, the plasmids were extracted and verified by single and double digestions. Thus, the recombinant plasmid pET21a-BvAmylase was obtained.

## 2.6. Prokaryotic Expression and Purification of the BvAmylase

For the detection of prokaryotic expression, a single clone of *E. coli* BL21 (DE3) cell containing pET21a-BvAmylase was picked and inoculated into 3 mL of LB + Amp (100 mg/L) medium, and cultured at 37 °C and 250 rpm for 12 h. Then, it was inoculated into LB liquid medium without antibiotics at the ratio of 1:100 (v/v), cultured at 37 °C and 250 rpm for 3 h ( $OD_{600} \approx 0.8$ ), and induced by 1 mM of IPTG at 37 °C. Simultaneously, the pET21a transformed BL21(DE3) strain was used as the control. After induction for 0, 2, 4, and 6 h, 2 mL of bacterial solution was collected and centrifuged at 4 °C and 9600× *g* for 1 min. The pellet was suspended with 100 µL of ddH<sub>2</sub>O and 25 µL of 5× sodium dodecyl sulfate-polyacrylamide gel electrophoresis (SDS-PAGE) loading buffer by vortexing, and boiled for 5 min. Twenty microliters of supernatant were taken for SDS-PAGE (5% concentrated gel and 12% separated gel) detection after centrifuged at 4 °C, 16,000× *g* for 5 min.

For the purification, 50 mL of the *E. coli* BL21(DE3) with pET21a-BvAmylase induced for 6 h was collected by centrifuging at 4 °C, 3500× *g* for 10 min, and the pellet was washed with 1× PBS (Na<sub>2</sub>HPO<sub>4</sub> 8 mM, NaCl 136 mM, KH<sub>2</sub>PO<sub>4</sub> 2 mM, KCl 2.6 mM, pH7.4) twice. Then, 5 mL of 1× PBS solution was added to suspend the pellet, and the cells were disrupted by Model 50 Sonic Dismembrator (Fisher Scientific, Pittsburgh, PA, USA). The supernatant and precipitate were separated by centrifuging at 4 °C, 16,000× *g* for 30 min. The *E. coli* BL21 (DE3) with the empty vector pET21a was the control. The amylase activity of both supernatants was measured by the DNS method at 40 °C. Meanwhile, SDS-PAGE was used to detect the supernatants for the target protein.

The supernatants with the BvAmylase were mixed and filtered with a 0.2 µm filter to remove impurities, and then was loaded into HisTrap HP column (GE Healthcare, Piscataway, NJ, USA) loaded with Ni<sup>2+</sup> and equilibrated with the binding buffer [sodium phosphate buffer (pH 7.4) 20 mM, NaCl 0.5 M, imidazole 5 mM] at the flow rate 1 mL/min. After washing with 10 mL of binding buffer [sodium phosphate buffer (pH 7.4) 20 mM, NaCl 0.5 M, imidazole 30 mM], the recombinant protein was washed with the elution buffer [sodium phosphate buffer (pH7.4) 20 mM, NaCl 0.5 M, imidazole 50/100/200/300/400/500 mM] sequentially, and the eluate was collected in 1.5 mL tube. The fractions were detected by nanodrop2000c at 280 nm and SDS-PAGE, separately. The eluted BvAmylase was mixed and dialyzed with 1× PBS at 4 °C overnight. Bradford reagent was used to quantify the purified amylase protein. Twenty microliters of amylase were added into 200 µL of Bradford reagent, mixed, and reacted at room temperature for 10 min, the absorption A<sub>595</sub> was recorded. Twenty microliters of ddH<sub>2</sub>O were taken as the control. The concentration of amylase was calculated by the BSA (Bovine Serum Albumin) standard curve.

## 2.7. Characterization of BvAmylase Enzyme

### 2.7.1. Effect of Temperature on BvAmylase Activity and Stability

The purified amylase was diluted 50 times by adding 20 µL of purified BvAmylase into 980 µL 1× PBS (pH 7.4). Then, the diluted BvAmylase was used for the following experiments. The optimum temperature of purified BvAmylase activity was explored by measuring the α-amylase activity at different temperatures (25, 30, 40, 50, 55, 60, 65, 70,

75, 80, 90, 100 °C) with the DNS method. Furthermore, the thermal stability of the purified amylase was obtained by preincubating the BvAmylase at different temperatures (40, 50, 60, 70, 80 °C) for 0–60 min, and then the activity was tested by the DNS method at optimum temperature. The results were calculated as the percentages of the highest activity reaction (100%).

#### 2.7.2. Effect of pH on BvAmylase Activity and Stability

Amylase activity was measured at optimum temperature using different buffers [0.1 M citric acid-sodium citrate (pH 4.0, 5.0, and 6.0), 0.1 M  $K_2HPO_4$ - $KH_2PO_4$  buffer (pH 7.0, 8.0, 9.0), and 0.1 M glycine-NaOH (pH 10.0, 11.0, 12.0)] for optimum pH. The enzyme was preincubated in varying pH (3.0–9.0) in the respective buffer for 48 h for the stability of purified BvAmylase. The residual enzyme activity was tested by the DNS method at optimum temperature. The results were calculated as the percentages of the highest activity reaction (100%).

#### 2.7.3. Effect of Some Metal Ions on BvAmylase Activity

The effect of metal ions ( $MnSO_4$ ,  $ZnSO_4$ ,  $FeSO_4$ ,  $CuSO_4$ , NaCl,  $CaCl_2$ , KCl,  $MgCl_2$ ,  $CoCl_2$ ) on purified BvAmylase activity was determined by preincubating the enzyme at room temperature for 30 min at 2 mM and 5 mM. The activity of the control without metals was taken as 100%. All assays were performed under optimum temperature and optimum pH as described above.

#### 2.7.4. Effect of Some Detergents and Organic Solvents on BvAmylase Activity

The effect of detergents (SDS, Triton X-100, and Tween 20) and organic solvents (methanol and ethanol) on purified BvAmylase activity was determined by preincubating the enzyme at room temperature for 30 min at 2% and 5% (w/v). The activity of the control without detergents and organic solvents was taken as 100%. All assays were performed under optimum temperature and optimum pH as described above.

#### 2.7.5. Determination of $K_m$ and $V_{max}$ for BvAmylase

The Michaelis constant ( $K_m$ ) is a basic characteristic constant of an enzyme, which reflects the binding and dissociation between enzyme and substrate. The initial velocities of the amylase activity were determined by the DNS method under optimum temperature and optimum pH. An amount of 70 ng (10  $\mu$ L) of purified amylase was added into 100  $\mu$ L of different starch concentration (0.15625, 0.3215, 0.625, 1.25, 2.5, 5, 10 mg/mL) in phosphate buffer (pH 6.0), gently mixed and incubated at 70 °C for 10 min. Then, 300  $\mu$ L of DNS was added and boiled in the water bath for 5 min. After cooling to room temperature, 200  $\mu$ L of the solution was taken into a 96-well plate, and the absorption was read at 540 nm. The reduced sugar produced after the reaction was calculated with a maltose standard curve. The initial velocities were expressed as  $\mu$ M maltose generated per minute per mg purified protein. The kinetic parameters  $K_m$  and  $V_{max}$  of the BvAmylase were obtained with non-linear regression function Michaelis Menten in software OriginPro 2018C.

#### 2.7.6. Bioinformatics of BvAmylase Gene

The nucleotide sequence was translated into a protein sequence by Genetyx version 6.1.8, and the BLASTp program of the NCBI website was used for sequence alignment, and DNAMAN version 7 was used for multisequence alignment. The Clustal W built-in MEGA X version 10.0.5 was used for the multisequence alignment, and then the Neighbor-Joining method was used to construct the phylogenetic tree with bootstrap = 1000. The conservative structural domain was predicted by Interpro software ([http://www.ebi.ac.uk/interpo/](http://www.ebi.ac.uk/interpro/), 18 June 2021). The hydrophobicity was analyzed by ProtScale software (<https://web.expasy.org/protscale/>, 18 June 2021). The secondary structure was predicted by SSpro software (<http://scratch.proteomics.ics.uci.edu/>, 18 June

2021). The three-dimensional model was calculated by SWISS-MODEL (<http://www.expasy.ch/swissmod/SWISS-MODEL.html>, 18 June 2021) and the obtained model was verified by ProSA [12].

2.7.7. Statistical Analysis

All data were analyzed using Microsoft Excel 2019 with one-way ANOVA. Data were described as mean values according to the results of at least three independent experiments, and SDs were presented as error bars. Data were considered as statistically significant for  $p \leq 0.05$ .

3. Results

3.1. Identification of WangLB Bacterium by 16S rDNA

The 16S rDNA of WangLB bacterium was amplified with its genomic DNA, and an approximately 1500 bp fragment was obtained (Figure 1). After T/A cloning, it was sequenced and deposited into GenBank (Accession number: MW015754).

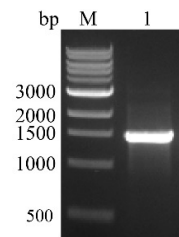


Figure 1. PCR result of 16S rDNA in WangLB bacterium. M: DNA marker. 1: PCR product.

BLAST results showed that the 16S rDNA of WangLB bacterium had the highest similarity with that of *Bacillus velezensis* strain FZB42. Phylogenetic analysis results indicated that WangLB and two *Bacillus velezensis* bacteria shared the same clade (Figure 2), which suggested that WangLB bacterium belonged to *Bacillus velezensis*.

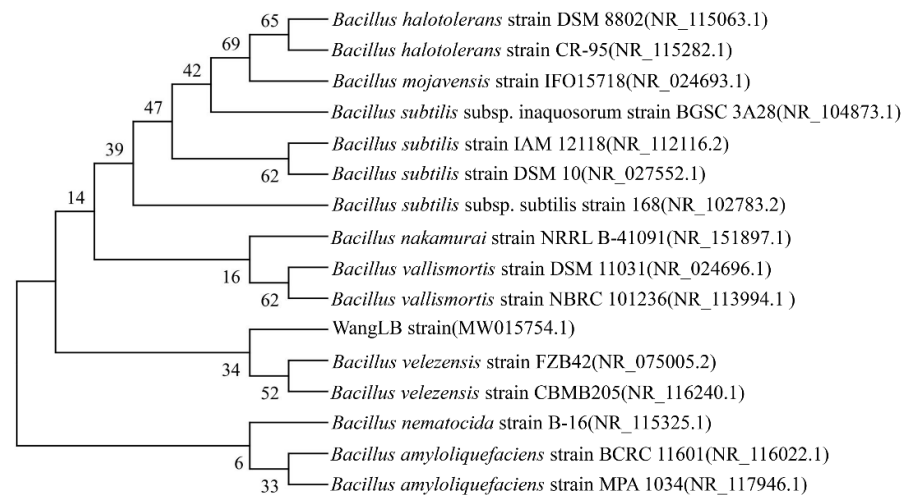


Figure 2. Phylogenetic analysis of the WangLB 16S rDNA with related bacteria. MEGA X was used and the maximum likelihood algorithm was selected to construct the tree with 1000 bootstraps and nucleotide Tamura-Nei substitution model.

### 3.2. Morphological and Biochemical Identification of WangLB

The single isolated colonies were observed on LB agar plate after 24 h of incubation. The morphology of the WangLB colonies was diameter 1–2 mm, grey, glossy, opaque, sticky texture, convex, neat, and smooth edge.

Enzyme activity, carbon source utilization, inhibition, and drug resistance of WangLB bacterium were measured by VITEK 2 BCL card. The results showed that it belonged to *Bacillus* as it had positive reactions in L-aspartate arylaminase, Leucine arylaminase, phenylalanine arylaminase, L-proline arylaminase, alanine arylaminase, tyrosine arylaminase, alanine phenylalanine proline arylaminase,  $\alpha$ -galactosidase [13],  $\beta$ -glucosidase, pyruvate, esculin hydrolysis, tetrazolium red, and resistance to polymyxin B (Table 1).

**Table 1.** Enzyme activity, carbon source utilization, inhibition, and drug resistance of WangLB bacterium.

Reaction Pore	Experiments	Abbreviation	Result
1	$\beta$ -Xylosidase	BXYL	–
3	L-lysine arylaminase	LysA	–
4	L-aspartate arylaminase	AspA	+
5	Leucine arylaminase	LeuA	+
7	Phenylalanine arylaminase	PheA	+
8	L-proline arylaminase	ProA	+
9	$\beta$ -galactosidase	BGAL	–
10	L-pyrrolidone arylaminase	PyrA	–
11	$\alpha$ -galactosidase	AGAL	+
12	Alanine arylaminase	AlaA	+
13	Tyrosine arylaminase	TyrA	+
14	$\beta$ -N-acetylglucosaminidase	BNAG	–
15	Alanine phenylalanine proline arylaminase	APPA	+
18	Cyclodextrin	CDEX	–
19	D-galactose	dGAL	–
21	Glycogen	GLYG	–
22	Inositol	INO	–
24	Methyl-a-D-glucopyranoside acidification	MdG	–
25	Ellman	ELLM	–
26	Methyl-d-xyloside	MdX	–
27	$\alpha$ -mannosidase	AMAN	–
29	Maltotriose	MTE	–
30	Glycine arylaminase	GlyA	–
31	D-mannitol	dMAN	–
32	D-mannose	dMNE	–
34	D-melezitose	dMLZ	–
36	N-acetyl-D-glucosamine	NAG	–
37	Palatinose	PLE	–
39	L-rhamnose	IRHA	–
41	$\beta$ -glucosidase	BGLU	+
43	$\beta$ -mannosidase	BMAN	–
44	Phosphorylcholine	PHC	–
45	Pyruvate	PVATE	+
46	$\alpha$ -glucosidase	AGLU	–
47	D-tagatose	dTAG	–
48	D-trehalose	dTRE	–
50	Inulin	INU	–
53	D-glucose	dGLU	–
54	D-ribose	dRIB	–
56	Putrescine assimilation	PSCNa	–
58	Growth in 6.5% NaCl	NaCl 6.5%	–
59	Kanamycin resistance	KAN	–
60	Oleandomycin resistance	OLD	–
61	Esculin hydrolysis	ESC	+
62	Tetrazolium Red	TTZ	+
63	Resistance to polymyxin B	POLYB R	+

Note: '+' indicates positive reaction while '-' denotes negative reaction.

### 3.3. Cloning, Sequence Analysis of the BvAmylase Gene, and Construction of the Prokaryotic Expression Plasmid

The *BvAmylase* gene from WangLB bacterium genomic DNA without stop codon was amplified, and about 2 000 bp fragment was obtained (Figure 3). After T/A cloning, it was inserted into the pUCm-T vector and sequenced.

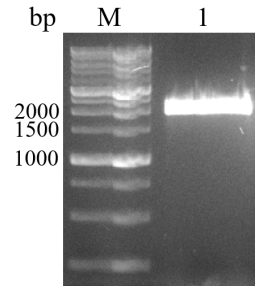


**Figure 3.** PCR result of the *BvAmylase* gene. M: DNA marker. 1: *BvAmylase* gene.

The sequencing results showed that the *BvAmylase* gene (accession number: MW822009) had a length of 1980 bp coding for 659 amino acids, and the relative molecular weight of *BvAmylase* protein was 72.35 kDa with its theoretical pI of 5.49. Sequence analysis results also showed *BvAmylase* protein belonged to the GH13 ( $\alpha$ -amylase) family and was a secretory protein. *BvAmylase* protein was a hydrophilic stable protein with a signal peptide (1–33 amino acids). The alignment results showed that *BvAmylase* shared 99.24%, 99.09%, and 98.03% of identity with  $\alpha$ -amylase from *Bacillus amyloliquefaciens* (WP\_174532725.1), *Bacillus velezensis* FZB42 (WP\_095273266.1), and *Bacillus subtilis* (AFD33644.1), respectively (Figure 4). The three conserved catalytic sites (D217, E249, D310) and the conserved  $Ca^{2+}$  binding sites (N142, D187, D212) were identified in *BvAmylase* which were identical to these  $\alpha$ -amylases (Figure 4).

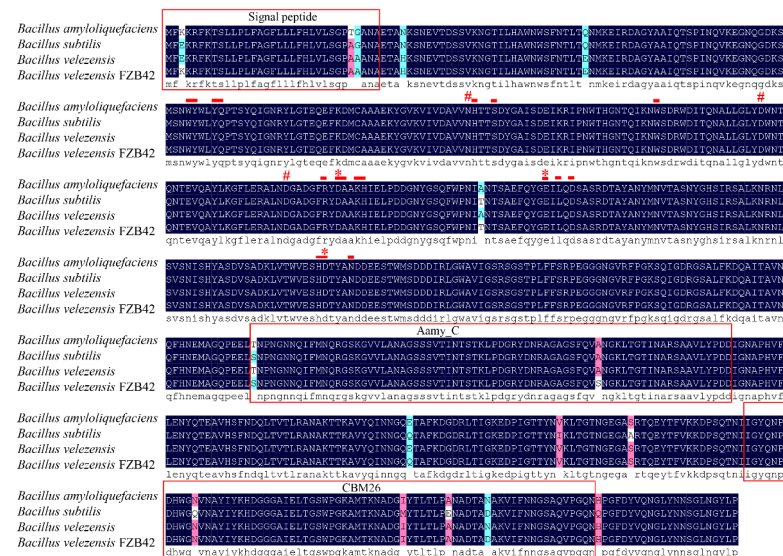


**Figure 4.** Alignment of *BvAmylase* and other  $\alpha$ -amylase proteins. DNAMAN 7 was used to perform the multi-sequence alignment. The signal peptide (1–33), C-terminal domain alpha-amylase (Amy\_C domain, 393–468), Starch-binding module 26 (CBM26, 565–636) is denoted by the red box. The active sites (99–100, 103–104, 143, 146, 171, 215, 217–218, 220–221, 249, 251, 253, 309–310, 314) are in the red line, the catalytic sites (217, 249, 310) are in asterisk, and  $Ca^{2+}$  binding sites (142, 187, 212) are in pound sign. Accession numbers for alpha-amylases are *Bacillus amyloliquefaciens* (WP\_174532725.1), *Bacillus subtilis* (AFD33644.1), *Bacillus velezensis* (MW822009, WangLB), and *Bacillus velezensis* FZB42 (WP\_095273266.1).



(QEE48109.1), *Olleya aquimaris* (AXO81475.1), *Flavobacterium johnsoniae* UW101 (ABQ04980.1), *Palaeococcus pacificus* DY20341 (AIF68502.1), *Thermococcus onnurineus* NA1 (ABA26948.1), *Pyrococcus furiosus* DSM 3638 (NP\_578206.1), *Thermococcus eurythermalis* (AIU69287.1), *Pyrococcus* sp. (BAA21130.1), *Thermococcus kodakarensis* (Q5JER7).

The three-dimensional (3D) model of BvAmylase was predicted using the  $\alpha$ -amylase template [1bag.1.A] of *Bacillus subtilis* and verified by the protein structure analysis tool ProSA. Results showed that the oligo state of BvAmylase was a monomer having 44 to 465 amino acids and sequence identity was 90.05%. BvAmylase model had three typical domains: Domain A was composed of the  $(\alpha/\beta)_8$  barrel with its catalytic residues, domain B was a long loop that protrudes the surface, and domain C was composed of eight anti-parallel beta-sheet structures (Figure 6A). The three conserved catalytic sites D217, E249, and D310 formed a pocket in the barrel of the A domain (Figure 6B). There were three  $\text{Ca}^{2+}$  binding sites N142, D187, and D212 near the barrel (Figure 6B). The binding of  $\text{Ca}^{2+}$  can stabilize the structure of the enzyme [14].

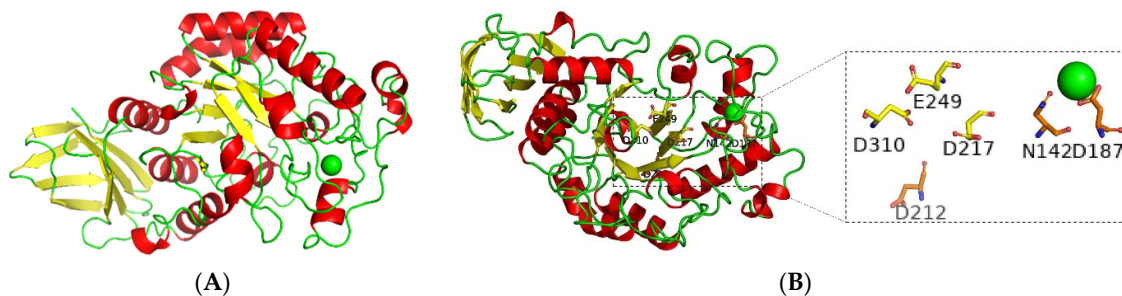


**Figure 6.** The homology structural model of the BvAmylase. (A) The structural model of the BvAmylase. The  $\alpha$ -helices,  $\beta$ -folds, and coils are shown in red, yellow, and green, respectively. (B) The conservative catalytic and  $\text{Ca}^{2+}$  binding sites. Residues of the catalytic triad are shown in yellow. The  $\text{Ca}^{2+}$  binding sites are shown in orange, while the  $\text{Ca}^{2+}$  is displayed as a green ball.

The digestion results showed that the total length of fragments generated by *Bam*HI and *Xho*I was equal to the single fragment length produced by *Bam*HI, which implied that the prokaryotic expression vector pET21a-BvAmylase was successfully constructed (Figure 7).

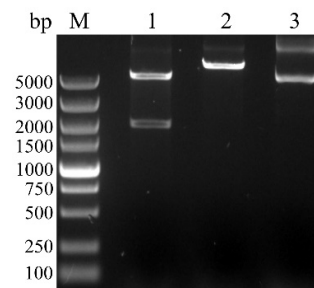


**Figure 7.** Verification of pET21a-BvAmylase by digestions. M: DNA standard. 1: Double digestion by *Bam*HI and *Xho*I. 2: Single digestion by *Xho*I; 3: Plasmid control.

### 3.4. Prokaryotic Expression and Purification of BvAmylase Gene of WangLB

To check whether the *BvAmylase* gene can be expressed or not, 1 mM of IPTG was used to induce the expression of BvAmylase overnight. The results showed that there was an expression at 2, 4, 6, and 24 h compared with the empty plasmid control (Figure 8).

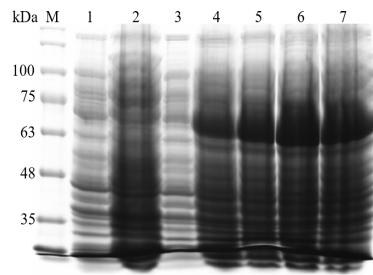


**Figure 8.** Induction of pET21a-BvAmylase expression. M: Protein standard; 1 and 2. BL21 (DE3) cells containing pET21a induced for 0 and 24 h; 3–7: BL21 (DE3) cells containing pET21a-BvAmylase induced for 0, 2, 4, 6, and 24 h.

For confirming the activity of the expressed BvAmylase, the supernatant of both the pET21a-BvAmylase cells and the control were tested for  $\alpha$ -amylase activity. The results showed high  $\alpha$ -amylase activity for the pET21a-BvAmylase, while only barely baseline for the control (Figure 9). Therefore, the supernatant of the pET21a-BvAmylase cell was used for further purification.

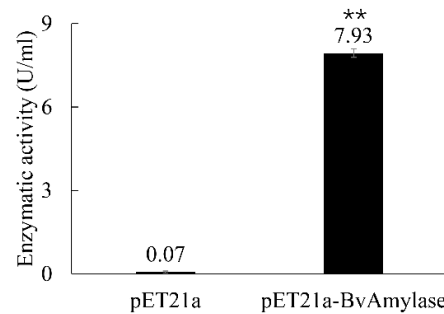


**Figure 9.** Detection of  $\alpha$ -amylase activity for BL21 (DE3) with pET21a-BvAmylase and pET21a. The BL21 cell with pET21a and pET21a-BvAmylase were induced for 24 h, collected, washed, disrupted, centrifuged, and the supernatants were used to measure the  $\alpha$ -amylase activity by the DNS method under 40 °C and 20 min. The experimental group was statistically different from the control experiment ( $p < 0.01$ ), as denoted by double asterisks.

The BL21 (DE3) cell with pET21a-BvAmylase and pET21a induced for 24 h were collected, ultrasonic disrupted, and centrifuged. The recombinant amylase was purified by nickel column. The SDS-PAGE results indicated that 200 mM of imidazole was the optimum washing concentration (Figure 10). To remove the imidazole, the elute of both 100 mM and 200 mM of imidazole were mixed and dialyzed with 1× PBS buffer at 4 °C overnight. Bradford method was used to quantify the concentration of purified amylase, the results showed that the purified amylase was about 350  $\mu$ g/mL.

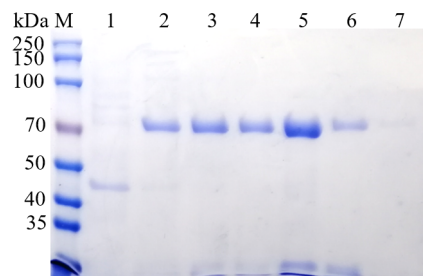


**Figure 10.** Detection of BvAmylase with SDS-PAGE. M: Protein standard. 1–7: The imidazole concentration is 1: 50, 2: 100, 3: 100, 4: 100, 5: 200, 6: 200, 7: 300 mM/L.

### 3.5. Characterization of BvAmylase of WangLB

#### 3.5.1. Effect of Temperature on the $\alpha$ -amylase Activity and Stability

BvAmylase showed more than 51.99% enzymatic activity from 40 °C to 75 °C, with its optimum temperature at 70 °C (Figure 11A). The results of thermostability experiments showed that BvAmylase was more stable at 40 °C and 50 °C, which had more than 63.93% activity after treatment for 60 min. With the increase in temperature, the enzymatic activity sharply decreased, when treated under 60 °C, 70 °C and 80 °C for 10 min, the enzymatic activity was 59.83%, 27.19%, and 6.01%, respectively; when extended for another 30 min, the enzymatic activity was 27.04%, 0%, and 0%, respectively (Figure 11B).

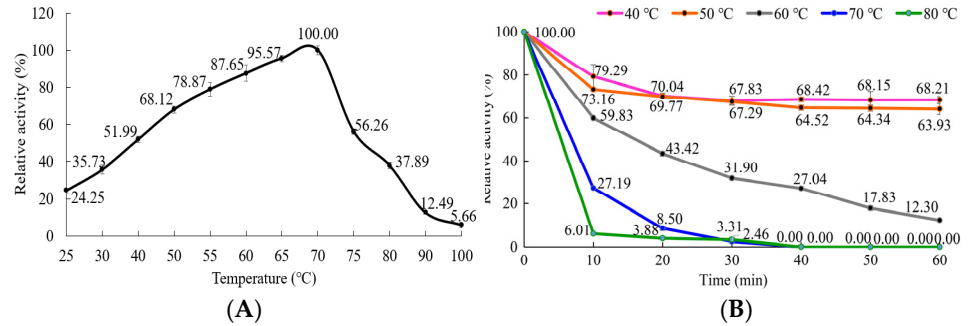


**Figure 11.** Effect of temperature on  $\alpha$ -amylase activity and stability. (A) Effect of temperature on  $\alpha$ -amylase activity. The optimum temperature of purified BvAmylase activity was determined by measuring the  $\alpha$ -amylase activity at different temperatures (25, 30, 40, 50, 55, 60, 65, 70, 75, 80, 90, 100 °C) with the DNS method. (B) Effect of temperature on  $\alpha$ -amylase stability. The purified BvAmylase was preincubated at different temperatures (40, 50, 60, 70, 80 °C) for 0–60 min, and then the activity was tested by the DNS method at optimum temperature. The highest activity and the activity without preincubating treatment were taken as control (100%). All assays were repeated four times. All of the experimental groups were statistically different from the control experiment ( $p < 0.01$ ).

#### 3.5.2. Effect of pH on the $\alpha$ -Amylase Activity and Stability

BvAmylase had good activity from pH5.0 (86.63%) to pH7.0 (69.05%) with optimum pH at pH6.0 (Figure 12A). After preincubation for 48 h, BvAmylase was more stable from pH6.0 (71.59%) to pH8.0 (86.60%) with the optimum pH7.0 (Figure 12B).

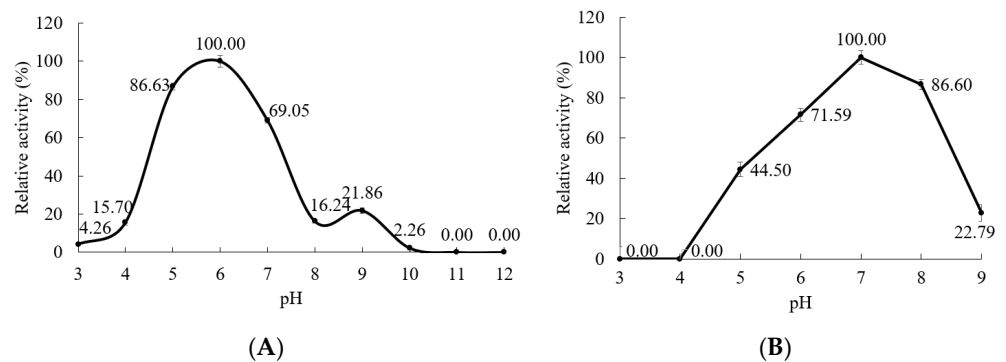


**Figure 12.** Effect of pH on  $\alpha$ -amylase activity and stability. (A) Effect of pH on  $\alpha$ -amylase activity. The  $\alpha$ -amylase activity was measured under 70 °C, 1% (w/v) starch, 20 min, and different pHs. (B) Effect of pH on  $\alpha$ -amylase activity and stability. The purified BvAmylase was preincubated in varying pH (3–9) in the respective buffer for 48 h, and the residual enzyme activity was tested by the DNS method. The highest activity and the highest residual activity were taken as the control (100%). All assays were repeated four times. All of the experimental groups were statistically different from the control experiment ( $p < 0.01$ ).

### 3.5.3. Influence of Metal Ions on the $\alpha$ -Amylase Activity

The effect of metal ions on BvAmylase was tested by measuring the activity in the presence of metal ions. The results showed that all of the metal ions tested ( $Mn^{2+}$ ,  $Zn^{2+}$ ,  $Fe^{2+}$ ,  $Na^+$ ,  $Ca^{2+}$ ,  $K^+$ ,  $Mg^{2+}$ ,  $Cu^{2+}$ ) inhibited the enzymatic activity of BvAmylase at both 2 mM and 5 mM except  $Co^{2+}$  which promoted the enzymatic activity at 2 mM and inhibited the enzymatic activity at 5 mM (Figure 13). The results also showed that BvAmylase was active without metal ions, suggesting it was a metal ion-independent enzyme. In general, the  $\alpha$ -amylase activity decreased as the concentration of metal ions increased. The activity of BvAmylase was reduced to 60.34%, 75.78%, and 79.76, respectively, when 2 mM  $Mn^{2+}$ ,  $Zn^{2+}$ , and  $Fe^{2+}$  were applied, and the activities were reduced to 38.43%, 46.21%, and 65.61% separately when the concentration increased to 5 mM (Figure 13). The enzymatic activity of BvAmylase was only slightly affected by 2 mM of  $Ca^{2+}$ ,  $K^+$ ,  $Mg^{2+}$ ,  $Cu^{2+}$ , however, 5 mM of those metal ions decreased the enzymatic activity by about 20%–30% compared to the control.

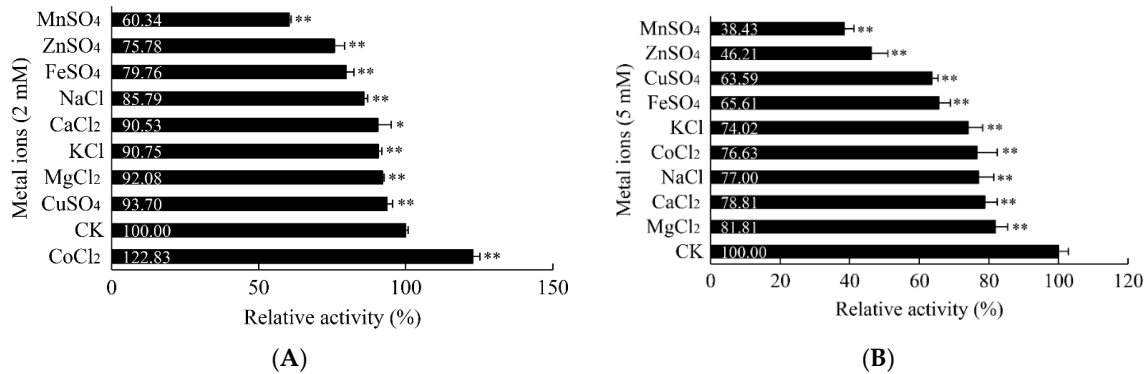


**Figure 13.** Influence of some metal ions on  $\alpha$ -amylase activity. (A) 2 mM. (B) 5 mM. The purified BvAmylase activity was determined by preincubating the enzyme with different metal ions ( $MnSO_4$ ,  $ZnSO_4$ ,  $FeSO_4$ ,  $CuSO_4$ ,  $NaCl$ ,  $CaCl_2$ ,  $KCl$ ,  $MgCl_2$ ,  $CoCl_2$ ) at room temperature for 30 min at 2 mM and 5 mM. The reaction activity without metal ions was taken as the control (CK), which was set to 100%. All assays were performed four times under 70 °C, pH 6.0, and 20 min. Single and double asterisks denoted the experimental groups were statistically different from the control experiment  $0.01 < p < 0.05$  and  $p < 0.01$ , respectively.

### 3.5.4. Influence of Detergents and Organic Solvents on $\alpha$ -Amylase Activity

The effect of detergents and organic solvents on BvAmylase was tested by measuring the activity in the presence of SDS, methanol, ethanol, Tween20, and Triton-X100. The results showed that SDS had the highest inhibiting activity on BvAmylase for which both 2% and 5% of SDS had reduced the enzymatic activity by more than 95% (Figure 14). For the ethanol and methanol, both of them reduced the enzymatic activity by about 10% at 2% and 5% concentration, separately. On the contrary, both Tween20 and Triton X-100 promoted the activity. Both 2% and 5% of Tween20 increased the enzymatic activity by 5.90% and 7.86%, while Triton X-100 increased by 14.97% and 31%, respectively (Figure 14). These results suggested that Triton X-100 can be used to stimulate the activity of BvAmylase.

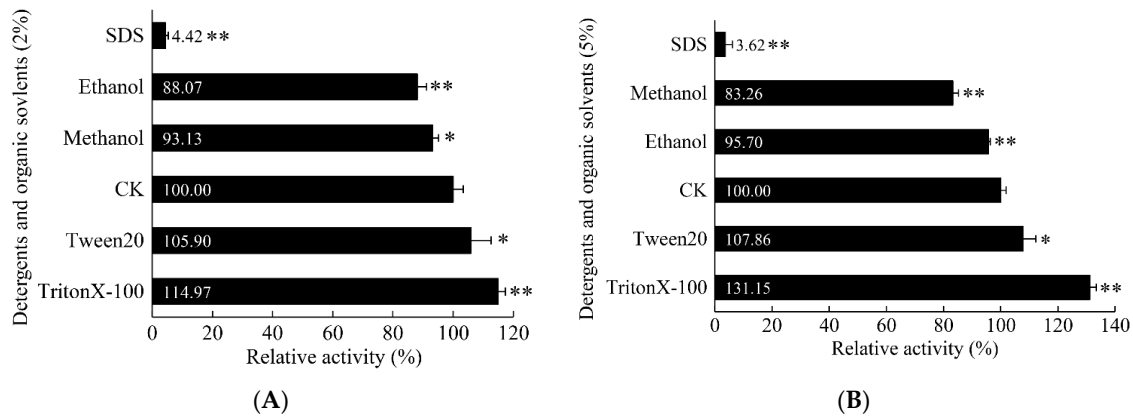


**Figure 14.** Influence of some detergents and organic solvents on BvAmylase activity. **(A):** 2% (w/v). **(B):** 5% (w/v). Conditions: 1% starch, pH6.0, 70 °C, 20 min. The purified BvAmylase activity was determined by preincubating the enzyme with detergents (SDS, Triton X-100, and Tween 20) and organic solvents (methanol and ethanol) at room temperature for 30 min at 2% (w/v) and 5% (w/v). The activity of the control without detergents and organic solvents was taken as 100%. All assays were performed four times at 70 °C, pH 6.0, and 20 min. Single and double asterisks denoted the experimental groups were statistically different from the control experiment  $0.01 < p < 0.05$  and  $p < 0.01$ , respectively.

### 3.5.5. Determination of the Kinetic Parameters of BvAmylase

By measuring the initial velocities of product generation, it was obvious to see BvAmylase complied with the Michaelis–Menten kinetics (Figure 15). The kinetic parameters  $K_m$  and  $V_{max}$  of the BvAmylase in the Michaelis–Menten equation were  $3.43 \pm 0.53$  mg/mL and  $434.19 \pm 28.57$  U/mg (Figure 14).

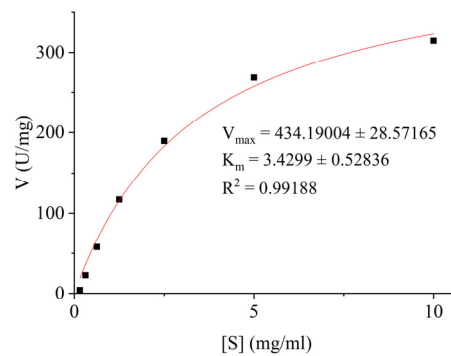


**Figure 15.** Saturation curve of varying starch concentration. The abscissa represents the starch concentration while the ordinate represents the velocity of reducing sugar yield. The initial velocities of the  $\alpha$ -amylase activity were determined by the DNS method under 70 °C, pH 6.0 and 20 min. All assays were repeated four times. The reduced sugar produced after the reaction was calculated with a maltose standard curve. The initial velocities were expressed as  $\mu$ M maltose generated per minute per mg purified protein. The kinetic parameters  $K_m$  and  $V_{max}$  of the BvAmylase were obtained by using the non-linear regression function Michaelis Menten in the software OriginPro 2018C.

## 4. Discussion

Amylase is one of the most indispensable enzymes which possess numerous applications in industries and laboratories [7]. According to the statistics, amylases comprise about 30% of the global market of industrial enzymes [15]. In industries,  $\alpha$ -amylase is mainly synthesized by bacteria and fungi. With the expansion of  $\alpha$ -amylase application, the demand is increasing year by year. Although a large number of  $\alpha$ -amylase has been identified and some of them have been used in production, the current enzymes cannot fully meet the industrial needs [16]. Recombinant DNA technology has been used to en-

hance the biosynthesis of  $\alpha$ -amylase [6]. With the aim of industrial production of  $\alpha$ -amylase, an  $\alpha$ -amylase-producing bacterium WangLB was identified, its  $\alpha$ -amylase coding gene was cloned, expressed, purified, and characterized.

In this study, we proposed that the WangLB strain was a new *Bacillus velezensis* species and the BvAmylase was a new  $\alpha$ -amylase. The evidences were: (1) although the analysis of the 16S rDNA showed the WangLB strain shared 99.60% identity with *Bacillus velezensis* strain FZB42, the biochemical reactions for esculin hydrolysis, tetrazolium red, and resistance to polymyxin B were all positive, which was different from the secondary metabolite cyclic lipopeptides (i.e., surfactin, bacillomycin-D, fengycin, and bacillibactin) and polyketides (i.e., macrolactin, bacillaene, and difficidin) synthesized by other *Bacillus velezensis* [17]. (2) the alignment result of the protein sequences showed BvAmylase shared 99.24% and 99.09% similarity with  $\alpha$ -amylase from *Bacillus amyloliquefaciens* and *Bacillus velezensis* FZB42 separately, however, they were not identical in the protein sequence.

The recombinant protein expression can be influenced by the expression vector, the host cell, the inducer, culture temperature, and the inducing time. For example, an organic-solvent-tolerant  $\alpha$ -amylase AmyH from *Exiguobacterium* sp. DAU5 was cloned into pET32a and expressed highest in *E. coli* BL21 (DE3) with 0.1 mM of IPTG at 30 °C and 5 h [18], while a halophilic  $\alpha$ -amylase gene EAMY from *E. coli* JM109 was cloned into the expression vector pSE380 and expressed highest with 1 mM of IPTG at 37 °C for 10 h [19]. Özcan et al. reported that the  $\alpha$ -amylase gene from *Bacillus stearothermophilus* was cloned into expression vector pETDuet-1 and expressed highest in *E. coli* BL21 (DE3) with 0.4 mM of IPTG at 37 °C and 18 h [20]. In this study, the  $\alpha$ -amylase gene *BvAmylase* was successfully cloned into pET21a, and highly expressed in *E. coli* BL21 (DE3) with 1 mM of IPTG at 37 °C and 6 h. However, Solat et al. inserted the thermo-tolerant halophilic  $\alpha$ -amylase AmyF into pET28b and expressed highest in *E. coli* BL21 (DE3) with higher than 0.1 mM of IPTG, and less activity was obtained due to the formation of a large number of inclusion bodies [21]. Instead of IPTG, the highest amount of the active recombinant  $\alpha$ -amylase AmyF was produced by 10 mM lactose for 8 h [21].

The relative molecular weight of  $\alpha$ -amylase varied among different bacteria. In this study, SDS-PAGE result showed that the relative molecular weight of BvAmylase was approximately 72.0 kDa, which was similar to the  $\alpha$ -amylase AmyJ33 (72.0 kDa) from *Bacillus amyloliquefaciens* JJC33M [22] and the  $\alpha$ -amylase AmyBS-1 (72.3 kDa) in *Bacillus subtilis* AS01a [23], was higher than the  $\alpha$ -amylase FMB1 (58.5 kDa) in *Anoxybacillus ayderensis* [5], the  $\alpha$ -amylase (52.0 kDa) in *Bacillus amyloliquefaciens* [24], the  $\alpha$ -amylase (56.0 kDa) in *Bacillus* sp. YX-1 [25] and the  $\alpha$ -amylase AMY1 (47.0 kDa) in *Massilia timonae* [6], however, was lower than the  $\alpha$ -amylase AmyKS (136.9 kDa) in *Bacillus subtilis* strain US572 [26] and the  $\alpha$ -amylase (85.0 kDa) in *Bacillus licheniformis* AT70 [27].

The optimal temperature of  $\alpha$ -amylase also varied among bacteria. The optimal temperature of BvAmylase was 70 °C which is identical to the  $\alpha$ -amylase from *Bacillus* sp. BCC021-50, *Nocardiopsis* sp., *Bacillus methylotrophicus* strain P11-2 and *Aspergillus* sp. [28–31]. The higher optimal temperature has been reported for a thermostable and acid-stable  $\alpha$ -amylase (100 °C) from *Bacillus licheniformis* B4-423, *Bacillus* sp. ANT-6 (80 °C), *Bacillus licheniformis* (80 °C) [32–34]. The lower optimal temperature has also been reported for  $\alpha$ -amylase in *Bacillus* sp. (35 °C) and *Tepidimonas fonticaldi* strain HB23 (35 °C), *Bacillus subtilis* MTCC 121 (40 °C) and *Halobacillus* sp. strain MA-2 (50 °C) [35–38]. Our BvAmylase displayed a wide range of thermal activity and the activity was 51.99% and 56.25% at 40 °C and 75 °C, respectively, indicating its applications in both medium-temperature and high-temperature processes in numerous industries.

The optimal pH of  $\alpha$ -amylase varied much between bacteria. BvAmylase exhibited the optimal activity at pH 6.0, and it was active at a narrow range of pH, displaying 86.63% and 69.05% activity at pH5.0 and pH7.0, respectively. These results were similar to AmyKS from *Bacillus subtilis* strain US572 with optimal pH 6.0 and showing 65.00% and 76.00% activity at pH 5.0 and pH 7.0, respectively [26]. Hence, this enzyme is suitable to be used in acidic conditions in industries. However,  $\alpha$ -amylase from WangLB, *B. subtilis*

JS-200449, and *Bacillus subtilis* showed the optimal activity at pH 9.0, pH 8.0, and pH 7.0, respectively [11,26,39]. In the literature, the optimal pH of  $\alpha$ -amylase from *Bacillus* was even ranged from 4.5 to 10.5 [14,40].

The effects of metal ions on  $\alpha$ -amylase activity are different between the source of organisms and in a concentration-dependent manner. The effects of metal ions on BvAmylase in our study have shown that it did not need any ions to activate its  $\alpha$ -amylase activity. The activity was decreased by increasing concentration of  $Mn^{2+}$ ,  $Zn^{2+}$ ,  $Fe^{2+}$ ,  $Ca^{2+}$ ,  $Mg^{2+}$ ,  $Cu^{2+}$ ,  $Na^+$ , and  $K^+$  from 2 mM to 5 mM (Figure 12). This is consistent with the  $\alpha$ -amylase for 2 mM of  $Zn^{2+}$  and  $Mg^{2+}$  in *Nesterenkonia* sp. strain F which reduces about 18% activity [21]. On the contrary,  $Cu^{2+}$  and  $Ca^{2+}$  did not decrease the  $\alpha$ -amylase activity and the highest  $\alpha$ -amylase activity was observed at 100 mM and 200 mM, respectively, for a pH and thermo-tolerant halophilic  $\alpha$ -amylase from moderate halophile *Nesterenkonia* sp. strain F [21]. For the  $\alpha$ -amylase in *Petrotoga mobilis*, 2 mM of  $Ca^{2+}$  increased the  $\alpha$ -amylase activity by about 10% while 5 mM of  $Ca^{2+}$  reduced the  $\alpha$ -amylase activity by about 10% [41]. For the  $\alpha$ -amylase from *Bacillus licheniformis* B4-423, both 1 mM and 5 mM of  $Ca^{2+}$ ,  $Mg^{2+}$ ,  $Na^+$ , and  $K^+$  did not affect the activity, however, both 1 mM (92.9%) and 5 mM (77.6%) of  $Mn^{2+}$  decreased the activity, while  $Zn^{2+}$ ,  $Co^{2+}$ ,  $Cu^{2+}$ , and  $Fe^{2+}$  severely inhibited the activity [32]. For the  $\alpha$ -amylase from Chinese Nong-flavor Daqu, both 1 mM and 10 mM of  $Zn^{2+}$  and  $Cu^{2+}$  decreased the  $\alpha$ -amylase activity by more than 95.0%, but  $Na^+$  and  $K^+$  just slightly decreased the activity [42]. For the  $\alpha$ -amylase from *Bacillus acidicola*, both 1 mM and 5 mM of  $Co^{2+}$  increased the activity by 150% and 130%, separately [43]. In this study, 2 mM of  $Co^{2+}$  increased the  $\alpha$ -amylase activity by 22.83%, and 5 mM of  $Co^{2+}$  decreased the  $\alpha$ -amylase activity by 23.37% (Figure 12). It can be explained by our proposed hypothesis: the  $Co^{2+}$  has a high affinity with the  $Ca^{2+}$ -binding sites, but a low affinity with the catalytic sites. When the concentration of  $Co^{2+}$  is 2 mM, it binds to the  $Ca^{2+}$ -binding sites to change the conformation of the catalytic center and to enhance the  $\alpha$ -amylase activity. On the contrary, when the concentration of  $Co^{2+}$  is 5 mM, not only it binds to the  $Ca^{2+}$ -binding sites to enhance the  $\alpha$ -amylase activity, but also binds to the catalytic center to inhibit the reaction, which is also competitive with the substrate soluble starch. Thus, the activity of  $\alpha$ -amylase decreases.

Most of the  $\alpha$ -amylases are metalloenzymes containing at least one  $Ca^{2+}$ -binding site by which to activate the enzymatic activity and structural stability [1]. In the  $Ca^{2+}$ -dependent  $\alpha$ -amylase, the metal triad  $Mg^{2+}$ - $Na^+$ - $Ca^{2+}$  in the main  $Ca^{2+}$ -binding site can link Domain A and B [44]. For our BvAmylase, both 2 mM and 5 mM of  $Ca^{2+}$  reduced the activity by 9.47% and 21.19% separately (Figure 12), suggesting it was a  $Ca^{2+}$ -independent  $\alpha$ -amylase which was suitable to be used in detergent industries. This is consistent with the  $\alpha$ -amylase from *Talaromyces pinophilus* 1-95, *Talaromyces pinophilus*, *Bacillus* sp. KR-8104 and *Bacillus licheniformis* B4-423 [32,45-47].

The detergents and the organic solvents also affected the  $\alpha$ -amylase activity. SDS is an anionic surfactant and a strong protein denaturant. For the  $\alpha$ -amylase from *Anoxybacillus ayderensis* FMB1, 0.04% (w/v) of SDS decreased the activity by 27% [5]. For the  $\alpha$ -amylase NFAmy13B from Chinese Nong-flavor Daqu, its activity was reduced by 96.78% and 97.98% under 0.03% (w/v) and 0.3% (w/v) of SDS, separately [42]. On the contrary, the anionic detergent 0.14% (w/v) of SDS did not inhibit the  $\alpha$ -amylase from *Massilia timonae*, while 0.28% (w/v) of SDS inhibited the activity by 17.50% [6]. For the  $\alpha$ -amylase from *Bacillus acidicola*, 0.1% of SDS did not change the activity while 0.2% (7.56 mM) reduced the activity by 10% [43]. It seemed that the lower concentration of SDS did not inhibit the  $\alpha$ -amylase activity and vice versa. In our study, both 2% (w/v) and 5% (w/v) of SDS severely reduced the  $\alpha$ -amylase activity by 95.58% and 96.38%, respectively, which was consistent with the  $\alpha$ -amylase from *Geobacillus* sp. GS33 that 1% (w/v) of SDS reduced the activity by 64% [48]. Therefore, the lower concentrations of SDS for BvAmylase should be tested in the future.

Tween 20 and Triton X-100 are mild non-ionic detergents. For the Tween 20, both 2% (w/v) and 5% (w/v) of which increased the BvAmylase activity by 5.90% and 7.86%, separately (Figure 13). This is consistent with the  $\alpha$ -amylase from a high maltose-forming, acid-stable, and  $\text{Ca}^{2+}$ -independent  $\alpha$ -amylase of the acidophilic *Bacillus acidicola* whose activity was increased by 16% for 0.2% (w/v) of Tween 20 [43]. In *Thalassobacillus* sp. LY18, 1.23% (w/v) of Tween 20 did not affect the activity of its  $\alpha$ -amylase at all [49]. In *Thermotoga petrophila* and *Geobacillus* sp. GS33, 1% (v/v) of Tween 20 decreased the  $\alpha$ -amylase activity by 13% and 34%, respectively [48,50]. In WangLB bacterium, both 2% (w/v) and 5% (w/v) of Tween 20 decreased the  $\alpha$ -amylase activity by about 14% and 32%, respectively [11]. In the case of Triton X-100, both 2% (w/v) and 5% (w/v) increased the BvAmylase activity by 14.97% and 31.15% (Figure 13), which was consistent with the  $\alpha$ -amylase from *Geobacillus* sp. GS33 where 1% (w/v) of Triton X-100 increased the activity by 28% [48]. However, the activity of the  $\alpha$ -amylase from the acidophilic *Bacillus acidicola* and *Thalassobacillus* sp. LY18 was not affected by 0.1% (w/v) and 0.65% (w/v) of Triton X-100, separately [43,49]. In WangLB bacterium, 2% (w/v) of Triton X-100 did not affect the activity while 5% (w/v) of that reduced the activity by about 12% [11].

Methanol and ethanol have a higher affinity with water, which can destroy the hydration membrane on the surface of  $\alpha$ -amylase and reduce the solubility of  $\alpha$ -amylase, then decrease the enzymatic activity. In this study, both methanol and ethanol slightly reduced the  $\alpha$ -amylase activity at 2% (w/v) and 5% (w/v) (Figure 13), which was consistent with the other  $\alpha$ -amylase isolated from WangLB [11].

$K_m$  represents the affinity between the substrate and the enzyme. In a previous study, the  $K_m$  and  $V_{max}$  of the secretory  $\alpha$ -amylase of WangLB were  $0.37 \pm 0.02$  mg/mL and 233.00 U/mg [11]. In this study, the  $K_m$  and  $V_{max}$  of BvAmylase were  $3.43 \pm 0.53$  mg/mL and  $434.19 \pm 28.57$  U/mg, which implied that our BvAmylase had a lower affinity with soluble starch than the previously isolated  $\alpha$ -amylase, however, it possessed higher activity than the previous one. We postulated that there were at least two  $\alpha$ -amylase existed in the WangLB bacterium, both of which accounted for the characteristic of the high  $\alpha$ -amylase production [11].

## 5. Conclusions

The high amylase-producing bacterium WangLB was identified as *Bacillus velezensis* according to the 16S rDNA and biochemical properties. The gene encoding an  $\alpha$ -amylase BvAmylase was cloned, prokaryotic expressed, purified, and characterized. *BvAmylase* gene had a length of 1980 bp, encoding 659 amino acids. The relative molecular weight and pI of BvAmylase were 72.35 kDa and 5.49, respectively. BvAmylase belonged to the GH13-5 family and possessed the conservative catalytic sites (D217, E249, and D310) and  $\text{Ca}^{2+}$ -binding sites, although it was a  $\text{Ca}^{2+}$ -independent enzyme. The optimum temperature and pH were 70 °C and pH 6.0, respectively. The BvAmylase was more stable at 40 °C and pH 7.0. All the tested metal ions inhibited the  $\alpha$ -amylase activity except for the 2 mM of  $\text{Co}^{2+}$ . Among the detergents used, SDS severely inhibited the activity while Tween 20 and Triton X-100 promoted the activity. Both methanol and ethanol inhibited the  $\alpha$ -amylase activity. The BvAmylase showed good activity at a broad temperature (40–75 °C) and a relatively narrow pH (5.0–7.0). The  $K_m$  and  $V_{max}$  of BvAmylase were  $3.43 \pm 0.53$  mg/mL and  $434.19 \pm 28.57$  U/mg, respectively. The clear classification of the WangLB strain, explicit *BvAmylase* gene sequence, the high  $\alpha$ -amylase activity of the recombinant enzyme, and its wide range of temperature convey its application potential in industries.

**Author Contributions:** Conceptualization, W.Q. and X.Z.; methodology, X.Z., C.L., and C.C.; formal analysis, X.Z., C.L., and X.C.; resources, W.Q.; data curation, X.Z. and C.L.; writing—original draft preparation, X.Z. and C.L.; writing—review and editing, W.Q., C.C., and S.S.; supervision, W.Q.; project administration, W.Q.; funding acquisition, W.Q., C.L., and X.Z. All authors have read and agreed to the published version of the manuscript.

**Funding:** This research was funded by the Natural Sciences and Engineering Research Council of Canada, grant number: RGPIN-2017-05366 to W.Q., Start-up Fund for Doctoral Scientific Research at Xuchang University, grant number: 20201009, 20201010 to C.L. and X.Z., and the China Scholarship Council, grant number: 201908530057 to X.Z.

**Data Availability Statement:** The accession numbers of 16S rDNA and BvAmulase gene for WangLB bacterium are MW015754 and MW822009, separately.

**Conflicts of Interest:** The authors declare no conflicts of interest.

## References

- Gupta, R.; Gigras, P.; Mohapatra, H.; Goswami, V.K.; Chauhan, B. Microbial  $\alpha$ -amylases: A biotechnological perspective. *Process Biochem.* **2003**, *38*, 1599–1616, doi:10.1016/S0032-9592(03)00053-0.
- van der Maarel, M.J.E.C.; van der Veen, B.; Uitdehaag, J.C.M.; Leemhuis, H.; Dijkhuizen, L. Properties and applications of starch-converting enzymes of the  $\alpha$ -amylase family. *J. Biotechnol.* **2002**, *94*, 137–155, doi:10.1016/S0168-1656(01)00407-2.
- Omemu, A.M.; Akpan, Bankole, M.D. Hydrolysis of raw tuber starches by amylase of *Aspergillus niger* AM07 isolated from the soil. *Afr. J. Biotechnol.* **2005**, *4*, 19–25, doi:10.5897/AJB2005.000-3006.
- Li, X.; Wang, Y.; Park, J.; Gu, L.; Li, D. An extremely thermostable maltogenic amylase from *Staphylothermus marinus*: *Bacillus* expression of the gene and its application in genistin glycosylation. *Int. J. Bio. Macromol.* **2018**, *107*, 413–417, doi:10.1016/j.ijbiomac.2017.09.007.
- Matpan Bekler, F.; Güven, K.; Gül Güven, R. Purification and characterization of novel  $\alpha$ -amylase from *Anoxybacillus ayderensis* FMB1. *Biocatal. Biotransfor.* **2020**, *39*, 322–332, doi:10.1080/10242422.2020.1856097.
- Tagomori, B.Y.; dos Santos, F.C.; Barbosa-Tessmann, I.P. Recombinant expression, purification, and characterization of an  $\alpha$ -amylase from *Massilia timonae*. *3 Biotech* **2021**, *11*, 13, doi:10.1007/s13205-020-02505-w.
- Farooq, M.A.; Ali, S.; Hassan, A.; Tahir, H.M.; Mumtaz, S.; Mumtaz, S. Biosynthesis and industrial applications of  $\alpha$ -amylase: A review. *Arch. Microbiol.* **2021**, *203*, 1281–1292, doi:10.1007/s00203-020-02128-y.
- Pinto, E.S.M.; Dorn, M.; Feltes, B.C. The tale of a versatile enzyme: Alpha-amylase evolution, structure, and potential biotechnological applications for the bioremediation of n-alkanes. *Chemosphere* **2020**, *250*, 126202, doi:10.1016/j.chemosphere.2020.126202.
- Janecek, S.; Svensson, B.; Henrissat, B. Domain evolution in the alpha-amylase family. *J. Mol. Evol.* **1997**, *45*, 322–331, doi:10.1007/pl00006236.
- Sahnoun, M.; Jemli, S.; Trabelsi, S.; Ayadi, L.; Bejar, S. *Aspergillus Oryzae* S2 alpha-Amylase domain C involvement in activity and specificity: In vivo proteolysis, molecular and docking studies. *PLoS ONE* **2016**, *11*, e0153868, doi:10.1371/journal.pone.0153868.
- Wang, S.; Jeyaseelan, J.; Liu, Y.; Qin, W. Characterization and optimization of amylase production in WangLB, a high amylase-producing strain of *Bacillus*. *Appl. Biochem. Biotechnol.* **2016**, *180*, 136–151, doi:10.1007/s12010-016-2089-5.
- Wiederstein, M.; Sippl, M.J. ProSA-web: Interactive web service for the recognition of errors in three-dimensional structures of proteins. *Nucleic Acids Res.* **2007**, *35*, W407–W410, doi:10.1093/nar/gkm290.
- Bhatia, S.; Singh, A.; Batra, N.; Singh, J. Microbial production and biotechnological applications of  $\alpha$ -galactosidase. *Int. J. Biol. Macromol.* **2020**, *150*, 1294–1313, doi:10.1016/j.ijbiomac.2019.10.140.
- Paul, J.S.; Gupta, N.; Belya, E.; Tiwari, S.; Jadhav, S.K. Aspects and recent trends in microbial alpha-amylase: A review. *Appl. Biochem. Biotechnol.* **2021**, *193*, 2649–2698, doi:10.1007/s12010-021-03546-4.
- Liu, X.; Kokare, C. Chapter 11 Microbial Enzymes of Use in Industry. In *Biotechnology of Microbial Enzymes*, Brahmachari, G., Ed.; Academic Press: Cambridge, MA, USA, 2017; pp. 267–298.
- van den Burg, B. Extremophiles as a source for novel enzymes. *Curr. Opin. Microbiol.* **2003**, *6*, 213–218, doi:10.1016/S1369-5274(03)00060-2.
- Rabbee, M.; Ali, M.; Choi, J.; Hwang, B.; Jeong, S.; Baek, K.H. *Bacillus velezensis*: A valuable member of bioactive molecules within plant microbiomes. *Molecules* **2019**, *24*, 1046, doi:10.3390/molecules24061046.
- Chang, J.; Lee, Y.S.; Fang, S.J.; Park, I.H.; Choi, Y.L. Recombinant expression and characterization of an organic-solvent-tolerant alpha-amylase from *Exiguobacterium* sp. DAU5. *Appl. Biochem. Biotechnol.* **2013**, *169*, 1870–1883, doi:10.1007/s12010-013-0101-x.
- Wei, Y.; Wang, X.; Liang, J.; Li, X.; Du, L.; Huang, R. Identification of a halophilic alpha-amylase gene from *Escherichia coli* JM109 and characterization of the recombinant enzyme. *Biotechnol. Lett.* **2013**, *35*, 1061–1065, doi:10.1007/s10529-013-1175-9.
- Zcan, D.; Spaholu, H.M. Simultaneous production of alpha and beta amylase enzymes using separate gene bearing recombinant vectors in the same *Escherichia coli* cells. *Turk. J. Biol.* **2020**, *44*, 201–207, doi:10.3906/biy-2001-71.
- Solat, N.; Shafiei, M. A novel pH and thermo-tolerant halophilic alpha-amylase from moderate halophile *Nesterenkonia* sp. strain F: Gene analysis, molecular cloning, heterologous expression and biochemical characterization. *Arch. Microbiol.* **2021**, *203*, 3641–3655, doi:10.1007/s00203-021-02359-7.
- Montor-Antonio, J.J.; Hernandez-Heredia, S.; Avila-Fernandez, A.; Olvera, C.; Sachman-Ruiz, B.; Del Moral, S. Effect of differential processing of the native and recombinant alpha-amylase from *Bacillus amyloliquefaciens* JJC33M on specificity and enzyme properties. *3 Biotech* **2017**, *7*, 336, doi:10.1007/s13205-017-0954-8.
- Gupta, N.; Belya, E.; Paul, J.S.; Tiwari, S.; Kunjam, S.; Jadhav, S.K. Molecular strategies to enhance stability and catalysis of extremophile-derived  $\alpha$ -amylase using computational biology. *Extremophiles* **2021**, *25*, 221–233, doi:10.1007/s00792-021-01223-2.

24. Demirkan, E.S.; Mikami, B.; Adachi, M.; Higasa, T.; Utsumi, S.  $\alpha$ -Amylase from *B. amyloliquefaciens*: Purification, characterization, raw starch degradation and expression in *E. coli*. *Process Biochem.* **2005**, *40*, 2629–2636, doi:10.1016/j.procbio.2004.08.015.
25. Liu, X.D.; Xu, Y. A novel raw starch digesting  $\alpha$ -amylase from a newly isolated *Bacillus* sp. YX-1: Purification and characterization. *Bioresour. Technol.* **2008**, *99*, 4315–4320, doi:10.1016/j.biortech.2007.08.040.
26. Salem, K.; Elgharbi, F.; Ben Hlima, H.; Perduca, M.; Sayari, A.; Hmida-Sayari, A. Biochemical characterization and structural insights into the high substrate affinity of a dimeric and  $\text{Ca}^{2+}$  independent *Bacillus subtilis* alpha-amylase. *Biotechnol. Prog.* **2020**, *36*, e2964, doi:10.1002/btpr.2964.
27. Afrisham, S.; Badoei-Dalfard, A.; Namaki-Shoushtari, A.; Karami, Z. Characterization of a thermostable,  $\text{CaCl}_2$ -activated and raw-starch hydrolyzing alpha-amylase from *Bacillus licheniformis* AT70: Production under solid state fermentation by utilizing agricultural wastes. *J. Mol. Catal. B: Enzym.* **2016**, *132*, 98–106, doi:10.1016/j.molcatb.2016.07.002.
28. Stamford, T.L.; Stamford, N.P.; Coelho, L.C.; Araujo, J.M. Production and characterization of a thermostable alpha-amylase from *Nocardiopsis* sp. endophyte of yam bean. *Bioresour. Technol.* **2001**, *76*, 137–141, doi:10.1016/s0960-8524(00)00089-4.
29. Xie, F.; Quan, S.; Liu, D.; Ma, H.; Li, F.; Zhou, F.; Chen, G. Purification and characterization of a novel  $\alpha$ -amylase from a newly isolated *Bacillus methylothrophicus* strain P11-2. *Process Biochem.* **2014**, *49*, 47–53, doi:10.1016/j.procbio.2013.09.025.
30. Aggarwal, R.; Dutta, T.; Sheikh, J. Extraction of amylase from the microorganism isolated from textile mill effluent via a vis desizing of cotton. *Sustain. Chem. Pharm.* **2019**, *14*, 100178, doi:10.1016/j.scp.2019.100178.
31. Simair, A.A.; Khushk, I.; Qureshi, A.S.; Bhutto, M.A.; Chaudhry, H.A.; Ansari, K.A.; Lu, C. Amylase production from thermophilic *Bacillus* sp. BCC 021-50 isolated from a marine environment. *Fermentation* **2017**, *3*, 25.
32. Wu, X.; Wang, Y.; Tong, B.; Chen, X.; Chen, J. Purification and biochemical characterization of a thermostable and acid-stable alpha-amylase from *Bacillus licheniformis* B4-423. *Int. J. Biol. Macromol.* **2018**, *109*, 329–337, doi:10.1016/j.ijbiomac.2017.12.004.
33. Deljou, A.; Arezi, I. Production of thermostable extracellular  $\alpha$ -amylase by a moderate thermophilic *Bacillus licheniformis* isolated from Qinarje Hot Spring (Ardebil prov. of Iran). *Period. Biol.* **2017**, *118*, 405–416, doi:10.18054/pb.v118i4.3737.
34. Burhan, A.; Nisa, U.; Gökhan, C.; Ömer, C.; Ashabil, A.; Osman, G. Enzymatic properties of a novel thermostable, thermophilic, alkaline and chelator resistant amylase from an alkaliphilic *Bacillus* sp. isolate ANT-6. *Process Biochem.* **2003**, *38*, 1397–1403, doi:10.1016/S0032-9592(03)00037-2.
35. Amoozegar, M.A.; Malekzadeh, F.; Malik, K.A. Production of amylase by newly isolated moderate halophile, *Halobacillus* sp. strain MA-2. *J. Microbiol. Methods* **2003**, *52*, 353–359, doi:10.1016/S0167-7012(02)00191-4.
36. Raul, D.; Biswas, T.; Mukhopadhyay, S.; Das, S.K.; Gupta, S. Production and partial purification of alpha amylase from *Bacillus subtilis* (MTCC 121) using solid state fermentation. *Biochem. Res. Int.* **2014**, *2014*, 568141, doi:10.1155/2014/568141.
37. Kannan, T.R.; Kanagaraj, C. Molecular characteristic of  $\alpha$ -AMYLASE enzymes producing from *Bacillus licheniformis* (JQ946317) using solid state fermentation. *Biocatal. Agri. Biotechnol.* **2019**, *20*, 101240, doi:10.1016/j.bcab.2019.101240.
38. Khusro, A.; Barathikannan, K.; Aarti, C.; Agastian, P. Optimization of thermo-alkali stable amylase production and biomass yield from *Bacillus* sp. under submerged cultivation. *Fermentation* **2017**, *3*, 7.
39. John Ravindar, D.; Elangovan, N. Molecular identification of amylase producing *Bacillus subtilis* and detection of optimal conditions. *J. Pharm. Res.* **2013**, *6*, 426–430, doi:10.1016/j.jopr.2013.04.001.
40. Haki, G.D.; Anceno, A.J.; Rakshit, S.K. Atypical  $\text{Ca}^{2+}$ -independent, raw-starch hydrolysing  $\alpha$ -amylase from *Bacillus* sp. GRE1: Characterization and gene isolation. *World J. Microbiol. Biotechnol.* **2008**, *24*, 2517–2524, doi:10.1007/s11274-008-9775-6.
41. Jabbour, D.; Sorger, A.; Sahm, K.; Antranikian, G. A highly thermoactive and salt-tolerant  $\alpha$ -amylase isolated from a pilot-plant biogas reactor. *Appl. Microbiol. Biotechnol.* **2013**, *97*, 2971–2978, doi:10.1007/s00253-012-4194-x.
42. Chen, L.; Yi, Z.; Fang, Y.; Jin, Y.; Zhao, H. Biochemical and synergistic properties of a novel alpha-mylase from Chinese nong-flavor Daqu. *Microb. Cell Fact.* **2021**, *20*, 80, doi:10.1186/s12934-021-01571-w.
43. Sharma, A.; Satyanarayana, T. Characteristics of a high maltose-forming, acid-stable, and  $\text{Ca}^{2+}$ -independent  $\alpha$ -amylase of the acidophilic *Bacillus acidicola*. *Appl. Biochem. Biotech.* **2013**, *171*, 2053–2064, doi:10.1007/s12010-013-0501-y.
44. Alikhajeh, J.; Khajeh, K.; Ranjbar, B.; Naderi-Manesh, H.; Lin, Y.H.; Liu, E.; Guan, H.H.; Hsieh, Y.C.; Chuankhayan, P.; Huang, Y.C.; et al. Structure of *Bacillus amyloliquefaciens* alpha-amylase at high resolution: Implications for thermal stability. *Acta Crystallogr. Sect. F Struct. Biol. Cryst. Commun.* **2010**, *66*, 121–129, doi:10.1107/S1744309109051938.
45. Sharma, A.; Satyanarayana, T. Microbial acid-stable  $\alpha$ -amylases: Characteristics, genetic engineering and applications. *Process Biochem.* **2013**, *48*, 201–211, doi:10.1016/j.procbio.2012.12.018.
46. Sajedi, R.H.; Naderi-Manesh, H.; Khajeh, K.; Ahmadvand, R.; Ranjbar, B.; Asoodeh, A.; Moradian, F. A Ca-independent  $\alpha$ -amylase that is active and stable at low pH from the *Bacillus* sp. KR-8104. *Enzyme Microb. Tech.* **2005**, *36*, 666–671, doi:10.1016/j.enzmictec.2004.11.003.
47. Liang, X.; Wang, F.; Luo, X.; Feng, Y.L.; Feng, J.X. Purification and characterization of a highly efficient calcium-independent  $\alpha$ -Amylase from *Talaromyces pinophilus* 1-95. *PLoS ONE* **2015**, *10*, e0121531, doi:10.1371/journal.pone.0121531.
48. Burhanoglu, T.; Sürmeli, Y.; Şanlı-Mohamed, G. Identification and characterization of novel thermostable  $\alpha$ -amylase from *Geobacillus* sp. GS33. *Int. J. Biol. Macromol.* **2020**, *164*, 578–585, doi:10.1016/j.ijbiomac.2020.07.171.
49. Li, X.; Yu, H.Y. Characterization of an organic solvent-tolerant alpha-amylase from a halophilic isolate, *Thalassobacillus* sp. LY18. *Folia Microbiol.* **2012**, *57*, 447–453, doi:10.1007/s12223-012-0160-3.
50. Zafar, A.; Aftab, M.N.; Din, Z.; Aftab, S.; Iqbal, I.; Haq, I. Cloning, purification and characterization of a highly thermostable amylase gene of *Thermotoga petrophila* into *Escherichia coli*. *Appl. Biochem. Biotechnol.* **2016**, *178*, 831–848, doi:10.1007/s12010-015-1912-8.